Available online at www.sciencedirect.com
SCIENCE DIRECT
Journal of Molecular Spectroscopy 236 (2006) 255–259
Journal of MOLECULAR SPECTROSCOPY
www.elsevier.com/locate/jms

Infrared emission spectroscopy of the $A^4\Phi_i$–$X^4\Delta_i$ and $B^4\Pi_i$–$X^4\Delta_i$ transitions of CoS

Shanshan Yu [a], Iouli E. Gordon [b], Phillip M. Sheridan [a], Peter F. Bernath [a,b,*]

[a] Department of Chemistry, University of Waterloo, Waterloo, Ont., Canada N2L 3G1
[b] Department of Physics, University of Waterloo, Waterloo, Ont., Canada N2L 3G1

Received 23 December 2005; in revised form 8 February 2006
Available online 20 March 2006

Abstract

The near-infrared emission spectrum of CoS has been recorded at a resolution of 0.04 cm^{-1} using a Fourier transform spectrometer. Gas-phase CoS was produced by the reaction of cobalt vapor and CS_2 vapor at about 3000 K in a carbon tube furnace. Two electronic transitions were observed for the first time in the 3200–6000 cm^{-1} region and have been assigned to the $A^4\Phi_i$–$X^4\Delta_i$ and $B^4\Pi_i$–$X^4\Delta_i$ transitions. The 0–0 bands for all four sub-bands of the $A^4\Phi_i$–$X^4\Delta_i$ transition, and the 0–0, 0–1, 1–0, and 1–1 bands for the 5/2–7/2 sub-band of the $B^4\Pi_i$–$X^4\Delta_i$ transition were rotationally analyzed. Combined with the previous microwave data from the literature, the present data were fitted using the usual Hund's case (c) energy level expressions, and spectroscopic constants were obtained for the $X^4\Delta_i$, $A^4\Phi_i$, and $B^4\Pi_i$ states of CoS. A Hund's case (a) fit was also carried out for the $A^4\Phi_i$–$X^4\Delta_i$ transition. The presence of a low-lying $^4\Phi_i$ state for both CoS and CoO was not anticipated based on previous experimental and theoretical work.

Keywords: Transition metal sulfides; Near-infrared electronic spectra; Fourier transform emission spectroscopy

1. Introduction

The electronic spectra of 3*d* transition metal oxides and sulfides are generally very complex. The metal atom often has many unpaired electrons that can produce a huge number of low-lying electronic states with high values of spin multiplicity and orbital angular momentum, as well as large spin–orbit interactions. These electronic states may perturb one other, thereby complicating their spectra and making analysis difficult. Theoretical calculations are plagued with similar problems and it is hard to predict the energy order and properties of the low-lying electronic states. Despite these difficulties, most of the 3*d* transition metal monoxides have been well studied partly due to their importance in astrophysics and as models in understanding the chemical bonding in simple metal systems [1]. In contrast, little data are available for the corresponding sulfides [2,3].

Theoretical calculations and isovalent arguments suggest that CoS has a similar order of electronic states as CoO [3,4]. The ground state of CoO has been established as $^4\Delta_i$ with an electron configuration of $\sigma^2\delta^3\pi^2$ by experiments [5–10] as well as theoretical calculations [3,11–14]. Three $^4\Delta$ states and two $^4\Phi$ states of CoO [8] have been identified by visible Doppler-limited intracavity spectroscopy and jet-cooling methods. A $^4\Pi_i$–$X^4\Delta_i$ transition of CoO has been observed in the near-infrared region by high-resolution Fourier transform spectroscopy [7] and it was suggested that a $^4\Sigma^-$ state should lie nearby because of the large Ω-doubling observed on some of the spin components of this $^4\Pi_i$ state. Four transitions have been reported in the near-infrared region for matrix-isolated CoO: one was assigned to the 0–0 band of the $^4\Pi_{5/2}$–$X^4\Delta_{7/2}$ sub-band, and three others were assigned tentatively to transitions involving $^4\Sigma^-$, $^6\Delta$, and $^2\Delta$ states, in the absence of gas-phase data [15]. Dolg et al. [11] predicted that the first excited state of CoO is a $^4\Sigma^-$ state and that it lies 0.5 eV (4032 cm^{-1}) above the $X^4\Delta_i$ ground state. Gutsev et al. [12] predicted that this $^4\Sigma^-$ excited state lies just 0.11 eV

* Corresponding author. Fax: +1 519 746 0435.
E-mail address: bernath@uwaterloo.ca (P.F. Bernath).

0022-2852/$ - see front matter © 2006 Elsevier Inc. All rights reserved.
doi:10.1016/j.jms.2006.02.004

(887 cm^{-1}) above the $X^4\Delta_i$ ground state. Using the B1LYP exchange-correlation functional, Uzunova et al. [13] calculated the properties of several excited states lying within 1 eV of the ground state, and predicted low-lying $^4\Sigma^-$, $^6\Delta$, and $^2\Delta$ states for CoO, but failed to predict low-lying $^4\Pi$ or $^4\Phi$ states. Using DFT and TDDFT methods, Dai et al. [14] predicted many low-lying excited states for CoO, such as $^4\Sigma^-$, $^4\Pi$, $^4\Phi$, $^4\Delta$, $^2\Pi$, $^2\Delta$, etc., but this paper does not provide unambiguous electronic assignments for most of these low-lying states. All of the above calculations predict a low-lying $^4\Sigma^-$ state with an internuclear distance shorter than that of the $X^4\Delta$ ground state.

The number of spectroscopic studies on CoS, however, is limited. An early ab initio calculation by Anderson et al. [16] predicted a $X^4\Sigma^-$ ground state, while later theoretical calculations by Bauschlicher and Maitre [3] and Bridgeman and Rothery [4] predicted a $X^4\Delta$ ground state. The only available experimental study on CoS is the microwave study by Flory et al. [2], in which the ground state of CoS was established as $^4\Delta_i$ with a $\sigma^2\delta^3\pi^2$ electron configuration.

The present paper reports on the first observation of two electronic transitions of CoS in the 3200–6000 cm^{-1} region, which have been assigned as the $A^4\Phi_i$–$X^4\Delta_i$ and $B^4\Pi_i$–$X^4\Delta_i$ transitions. A rotational analysis of the 0–0 bands for all four sub-bands of the $A^4\Phi_i$–$X^4\Delta_i$ transition, and the 0–0, 0–1, 1–0, and 1–1 bands for the 5/2–7/2 sub-band of the $B^4\Pi_i$–$X^4\Delta_i$ transition is described and discussed.

2. Experimental

Gas-phase CoS was produced by the reaction of cobalt vapor and CS_2 vapor. Cobalt vapor was obtained by heating cobalt metal to about 3000 K in a carbon tube furnace (King furnace). A mixture of ~150 Torr He and ~30 mTorr CS_2 vapor was present in the furnace. The emission from CoS was focused using a CaF_2 lens into the entrance aperture of a Bruker IFS 120 HR Fourier transform spectrometer.

The near-infrared spectrum of CoS was measured at a resolution of 0.04 cm^{-1} in the 1800–8000 cm^{-1} region using a CaF_2 beamsplitter and a liquid nitrogen-cooled InSb detector, with a total recording time of about one hour (80 scans). The spectrum also contained strong emission lines from impurities (CO, HF, and HCl), which were used for calibration. The accuracy of the CoS line positions is estimated to be approximately 0.005 cm^{-1}.

3. Results and discussion

The program WSPECTRA, written by M. Carleer (Université Libre de Bruxelles), was used to determine the line positions, and a color Loomis–Wood program was used to pick out the branches. The CoS bands assigned to the $A^4\Phi_i$–$X^4\Delta_i$ transition were observed in the 3200–4000 cm^{-1} spectral region as shown in Fig. 1. A $^4\Phi_i$–$^4\Delta_i$ transition should consist of four sub-bands: $^4\Phi_{9/2}$–$^4\Delta_{7/2}$, $^4\Phi_{7/2}$–$^4\Delta_{5/2}$, $^4\Phi_{5/2}$–$^4\Delta_{3/2}$, and $^4\Phi_{3/2}$–$^4\Delta_{1/2}$. For Hund's case (a) states, these four sub-bands should be separated by the difference between the spin–orbit separations of the upper and lower states. We observed four unevenly spaced bands with R heads near 3414, 3670, 3827, and 3925 cm^{-1} (Fig. 1) and the lower states of these bands were confirmed to be the $v = 0$ levels of the four spin components of the $X^4\Delta_i$ ground state using lower state combination differences from the microwave study [2]. The three strongest sub-bands show clear single P, Q, and R branches, while the weakest sub-band shows two P, two Q, and two R branches. The Q branch is much stronger than the P and R branches in each of these sub-bands, indicating that these sub-bands are perpendicular transitions ($\Delta\Omega = \pm 1$) arising from either a $^4\Phi_i$–$^4\Delta_i$ transition or a $^4\Pi_i$–$^4\Delta_i$ transition. As the Ω-doubling splitting is small and present only in one of the four sub-bands, we assign these observations to the four sub-bands of the 0–0 band of a $^4\Phi_i$–$^4\Delta_i$ transition. It is interesting to note that this low-lying $^4\Phi_i$ state has not yet been assigned in the isovalent CoO molecule [7,8,15].

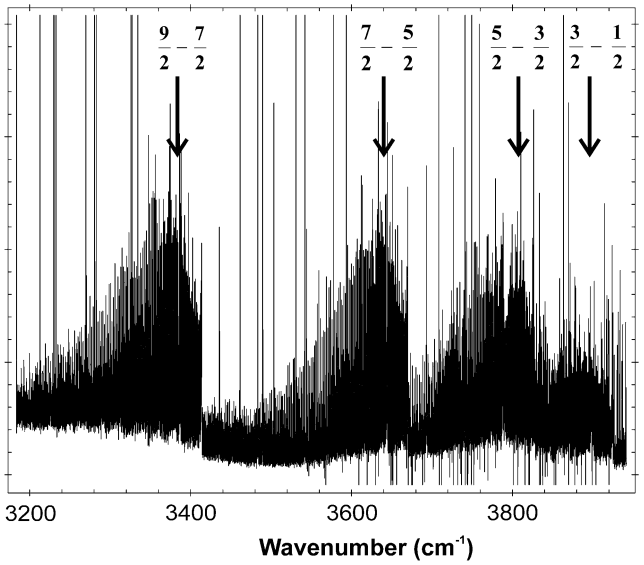

Fig. 1. An overview of the 0–0 band of the $A^4\Phi_i$–$X^4\Delta_i$ transition in CoS recorded at a resolution of 0.04 cm^{-1}. Four unevenly spaced sub-bands with strong R heads are present and arise from the $\frac{9}{2}-\frac{7}{2}$, $\frac{7}{2}-\frac{5}{2}$, $\frac{5}{2}-\frac{3}{2}$, and $\frac{3}{2}-\frac{1}{2}$ sub-bands. Perturbations were observed in the $\frac{5}{2}-\frac{3}{2}$ sub-band (see text). The strong emission lines are from the impurity HF.

Three additional bands, with R heads near 5147, 5624, and 4634 cm^{-1}, are also observed for CoS and are shown in Fig. 2. These features were assigned as the 0–0, 1–0, and 0–1 bands of the 5/2–7/2 sub-band of the $B^4\Pi_i$–$X^4\Delta_i$ transition. Rotational assignments were made using lower state combination differences. The 1–1 band was then predicted and identified in the spectrum. Fig. 3 shows an expanded view of the 0–0 band. The other two vibrational sub-bands have similar structure. The spectrum is very dense and lines from different branches overlap with each other. The Ω-doubling splitting in these bands begins to be resolved at $J \approx 60$. Weak bands with R heads near 4645, 4646, 4891, 4899, 5260, and 5262 cm^{-1}, as shown

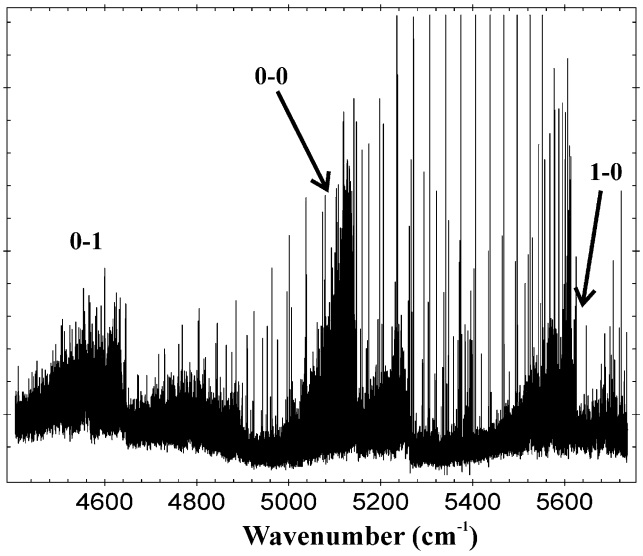

Fig. 2. An overview of the $B^4\Pi_i$–$X^4\Delta_i$ transition of CoS recorded at a resolution of 0.04 cm^{-1}. The 0–0, 0–1, and 1–0 bands of the $^4\Pi_{5/2}$–$X^4\Delta_{7/2}$ sub-band are labeled. The 1–1 band was also identified, but not marked in this figure. Additional weak bands are present in this region, and probably arise from other sub-bands of the $B^4\Pi_i$–$X^4\Delta_i$ transition. However, these bands could not be assigned due to their weak intensity. The spectrum also contained strong emission lines from the impurity HF, which were used for calibration.

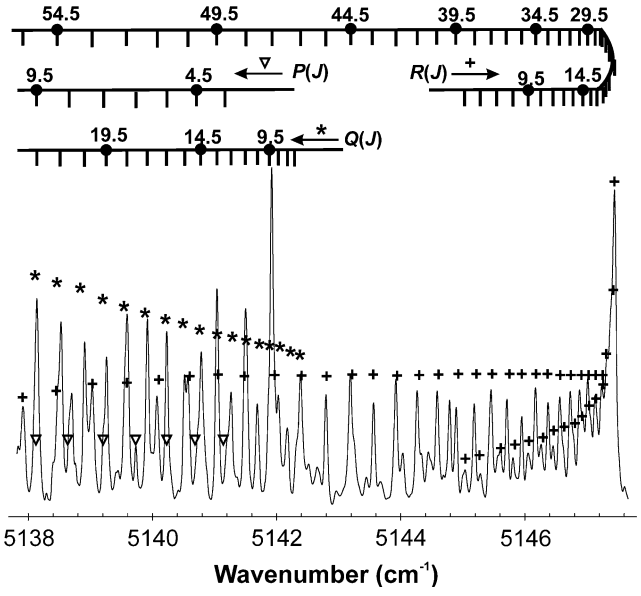

Fig. 3. An expanded view of the 0–0 band of the $B^4\Pi_{5/2}$–$X^4\Delta_{7/2}$ sub-band of CoS. A strong R branch head is present. Rotational assignments are shown above the spectrum. The spectrum is very dense and lines from different branches overlap with each other. The Ω-doubling, which is resolved starting at $J \approx 60$, is not shown.

in Fig. 2, could not be rotationally assigned because of their relatively weak intensity. Some of these bands probably arise from the $\frac{3}{2}-\frac{5}{2}$, $\frac{1}{2}-\frac{3}{2}$, and $(-\frac{1}{2})-\frac{1}{2}$ sub-bands of the $B^4\Pi_i$–$X^4\Delta_i$ transition. The analogous low-lying $^4\Pi_i$ state has been observed in CoO [7,8,15].

For data analysis we first performed Hund's case (c) fits for the observed bands. The usual empirical energy level expression was used for each of the spin components of the $X^4\Delta_i$, $A^4\Phi_i$, and $B^4\Pi_i$ states:

$$(J) = T_v + B_v J(J+1) - D_v[J(J+1)]^2 \pm 1/2[p_v(J+1/2) + p_{D_v}(J+1/2)^3 + p_{H_v}(J+1/2)^5 + p_{L_v}(J+1/2)^7], \quad (1)$$

in which the upper (lower) sign refers to $e(f)$ parity, and p_v, p_{D_v}, p_{H_v}, and p_{L_v} are Ω-doubling constants. The e- and f-parity assignments were arbitrarily chosen for bands with resolved Ω-doubling. The Hund's case (c) spectroscopic constants obtained for CoS are provided in Table 1. Lines from the 0–0, 1–1, 0–1, and 1–0 bands of the $B^4\Pi_{5/2}$–$X^4\Delta_{7/2}$ sub-band, and the 0–0 band of the $A^4\Phi_{9/2}$–$X^4\Delta_{7/2}$ sub-band were fitted together because they are all connected. The output file of this fit is provided in the supplementary Table S1. The 0–0 bands of the $\frac{7}{2}-\frac{5}{2}$, $\frac{5}{2}-\frac{3}{2}$, and $\frac{3}{2}-\frac{1}{2}$ sub-bands of the $A^4\Phi_i$–$X^4\Delta_i$ transition were fitted separately and the output files of these fits are provided in the supplementary Tables S2, S3, and S4, respectively. An estimated uncertainty of 0.005 cm^{-1} was used for most lines, and an uncertainty of 0.05 cm^{-1} was used for blended lines near band origins and band heads. The hyperfine-free pure rotational line positions in the four spin components of the $X^4\Delta_i$ state (extracted using the data published in [2]) were also included in the fits.

For the $^4\Phi_{9/2}$–$^4\Delta_{7/2}$ and $^4\Phi_{7/2}$–$^4\Delta_{5/2}$ sub-bands, lines with J'' up to 160 were assigned, and for the $^4\Phi_{3/2}$–$^4\Delta_{1/2}$ sub-band which has resolved Ω-doubling, lines with J'' up to 80 were assigned. However, strong perturbations were observed in the 0–0 band of the $^4\Phi_{5/2}$–$^4\Delta_{3/2}$ sub-band. As a result, only lines with $J'' < 60$ could be assigned and lines with $J'' > 40$ were deweighted to obtain a successful fit. In addition, there are many strong lines observed in the region in which the $A^4\Phi_{5/2}$–$X^4\Delta_{3/2}$ sub-band high J lines are expected (Fig. 1), but we could not assign these lines. Due to the perturbations, a relatively large value was obtained for the D_0 centrifugal constant (1.845×10^{-7} cm^{-1}) for the $A^4\Phi_{5/2}$ spin component (Table 1), as compared to the other spin components of the $A^4\Phi_i$ state. Based only on the observations in this experiment, we were unable to identify the source of these perturbations.

As given in Table 1, the 0–0, 1–1, 0–1, and 1–0 bands of the $B^4\Pi_{5/2}$–$X^4\Delta_{7/2}$ sub-band required p_H and p_L Ω-doubling constants for the $B^4\Pi_{5/2}$ spin component. The Ω-doubling splitting increases as $\sim J^5$ and is present entirely in the $B^4\Pi_{5/2}$ spin component. In the fit for the 0–0 band of the $A^4\Phi_{3/2}$–$X^4\Delta_{1/2}$ sub-band, only p and p_D were needed for the $X^4\Delta_{1/2}$ spin component, where the Ω-doubling splitting increases linearly with J. The spectroscopic constants in Table 1 provide vibrational intervals $\Delta G_{1/2} = 514.55244(31)$ cm^{-1} for the $X^4\Delta_{7/2}$ spin component, and $\Delta G_{1/2} = 476.82124(44)$ cm^{-1} for the $B^4\Pi_{5/2}$ spin component. Equilibrium constants $B_e = 0.20773952(23)$ cm^{-1}, $\alpha_e = 0.00010672(23)$ cm^{-1}, $r_e = 1.9786450(11)$ Å were determined for the $X^4\Delta_{7/2}$ spin component, while $B_e = 0.19903466(81)$ cm^{-1}, $\alpha_e = 0.00104903(81)$ cm^{-1},

Table 1
Hund's case (c) constants (in cm^{-1}) for the $X^4\Delta_i$, $A^4\Phi_i$, and $B^4\Pi_i$ states of CoS (all uncertainties are 1σ)

State	T_v	B_v	D_v (10^{-7})	p_v (10^{-3})	p_{Dv} (10^{-9})	p_{Hv} (10^{-10})	p_{Lv} (10^{-13})
$X^4\Delta_{7/2}$, $v=0$	0	0.207205911(46)	1.33499(15)				
$X^4\Delta_{7/2}$, $v=1$	514.55244(31)	0.20613870(23)	1.33990(79)				
$A^4\Phi_{9/2}$, $v=0$	3408.92170(51)	0.19911315(11)	1.31204(16)				
$B^4\Pi_{5/2}$, $v=0$	5142.73509(43)	0.19851015(39)	1.23015(68)	—	—	0.476(28)	−0.2141(52)
$B^4\Pi_{5/2}$, $v=1$	5619.55633(45)	0.19746112(71)	1.1925(23)	—	—	2.31(12)	−1.478(41)
$X^4\Delta_{5/2}$, $v=0$	0	0.207666544(41)	1.35157(15)				
$A^4\Phi_{7/2}$, $v=0$	3665.04287(42)	0.199226807(94)	1.31806(16)				
$X^4\Delta_{3/2}$, $v=0$	0	0.207934000(57)	1.35742(39)				
$A^4\Phi_{5/2}$, $v=0$	3821.9041(14)	0.1993555(26)	1.845(11)				
$X^4\Delta_{1/2}$, $v=0$	0	0.208226134(38)	1.36260(14)	−3.9383(28)	−8.06(93)	—	—
$A^4\Phi_{3/2}$, $v=0$	3920.56439(56)	0.19952061(34)	1.34676(44)				

$r_e = 2.0214505(39)$ Å were obtained for the $B^4\Pi_{5/2}$ spin component.

As we observed all four spin components of the $X^4\Delta_i$ and $A^4\Phi_i$ states in CoS, we also performed a Hund's case (a) fit for the 0–0 band of the $A^4\Phi_i$–$X^4\Delta_i$ transition. The observed lines were fitted to the usual $\hat{N}^2$ Hamiltonian for $^4\Delta$ and $^4\Phi$ states as given by Brown et al. [17]. An explicit listing of the matrix elements are provided by Brown et al. [18] for $^4\Delta$ states and by Ram et al. [19] for $^4\Phi$ states. The output file of this fit is provided in the supplementary Table S5. The spectroscopic constants obtained are given in Table 2. We could not determine the spin–orbit constant A and spin–spin constant λ for the $X^4\Delta_i$ ground state and they were fixed at the values from the previous microwave study [2]. As no transitions that cross spin components were observed, the Hund's case (a) constants obtained here are not very reliable (especially the A, λ, and η constants). At this moment, we prefer the constants obtained from the Hund's case (c) fit for CoS.

The $^4\Phi_i$–$^4\Delta_i$ transition is a fully allowed transition with $\Delta\Lambda = +1$ and $\Delta S = 0$, and in our experiments on CoS, the $A^4\Phi_i$–$X^4\Delta_i$ transition was stronger than the $B^4\Pi_i$–$X^4\Delta_i$ transition. Ram et al. [7] did not observe the analogous $^4\Phi_i$–$^4\Delta_i$ transition in their study of CoO because they used a green glass filter, which cuts off the spectral region where this transition should be found. Surprisingly, this $^4\Phi_i$–$^4\Delta_i$ transition in CoO was not assigned in the matrix isolation study by Danset and Manceron [15], in which four electronic transitions were observed in the near-infrared region: the strongest transition at 5887 cm^{-1} was assigned to the 0–0 band of the $^4\Pi_{5/2}$–$X^4\Delta_{7/2}$ sub-band, and the other three weaker transitions at 3377, 7010, and 10162 cm^{-1} were tentatively assigned to $^4\Sigma^-$–$X^4\Delta_{7/2}$, $^6\Delta$–$X^4\Delta_{7/2}$, and $^2\Delta$–$X^4\Delta_{7/2}$ transitions, respectively. Attempts to generate the CoO molecule with our carbon tube furnace and to record its spectrum in the near-infrared region were made, but failed. The most likely reason is that CoO was reduced to Co by carbon at high temperature [20]. Investigations of CoO using other experimental methods, such as a hollow cathode lamp, are desirable to locate the expected $^4\Phi$ state with an energy of about 4000 cm^{-1} based on CoS. Indeed, it is likely that the $^4\Phi_{9/2}$ spin component has already been located (but misassigned) in matrix isolation experiments of Danset et al. [15]. The $^4\Sigma^-_{3/2}$–$X^4\Delta_{7/2}$ transition is expected to be strongly forbidden ($\Delta\Omega = 2$) and appear rather weakly (if at all) in the matrix absorption spectrum. We therefore tentatively reassign this CoO transition at 3377 cm^{-1} in a neon matrix to the $A^4\Phi_{9/2}$–$X^4\Delta_{7/2}$ transition.

The $X^4\Delta_i$ ground states of CoO and CoS have been determined to arise from a $\sigma^2\delta^3\pi^2$ electron configuration [2,5–10], and the $X^4\Delta_i$ ground states of CoO and CoS have been found to have similar ^{59}Co nuclear hyperfine splittings [2,10]. Ram et al. [7] suggested that the $A^4\Pi_i$ state of CoO arises from a mixture of two configurations ($\sigma^2\delta^2\pi^3$ and $\sigma^1\delta^3\pi^3$) based on observations of anomalous lineshapes in the $A^4\Pi_{5/2}$–$X^4\Delta_{7/2}$ sub-band. These anomalous lineshapes were assigned to partly resolved ^{59}Co nuclear hyperfine structure in the $A^4\Pi_{5/2}$ state. We did not observe any anomalous lineshapes in the $A^4\Phi_i$–$X^4\Delta_i$ and $B^4\Pi_i$–$X^4\Delta_i$ transitions in CoS. It is more likely that the $B^4\Pi_i$ state in CoS arises solely from the $\sigma^2\delta^2\pi^3$ configuration since the $\sigma^1\delta^3\pi^3$ configuration with an unpaired electron in the Co 4s orbital would give rise to states with a large Fermi contact hyperfine parameter (b_F) and large magnetic hyperfine splittings. One possible reason for no observation of hyper-

Table 2
Hund's case (a) constants (in cm^{-1}) for the $X^4\Delta_i$ and $A^4\Phi_i$ states of CoS

Constant	$X^4\Delta_i$		$A^4\Phi_i$
	Present work	Microwave[a]	Present work
T_0	0	0	3704.13298(32)
A_0	−160.3[b]	−160.3(11)	−163.141624(66)
$A_{D0}/10^{-5}$	−2.62379(29)	−2.652(97)	1.3282(38)
B_0	0.207759165(17)	0.207759119(20)	0.19927642(27)
$D_0/10^{-7}$	1.351809(66)	1.351480(87)	1.319618(68)
$p_0/10^{-9}$	−3.94(57)	−4.00(60)	—
$o_0/10^{-6}$	−1.83(15)	−1.86(13)	—
$n_0/10^{-4}$	−6.5645(43)	−6.5632(37)	—
λ_0	22.3[b]	22.28(93)	2.60388(15)
$\lambda_{D0}/10^{-5}$	3.75701(38)	3.55(22)	2.028(13)
$\lambda_{H0}/10^{-11}$	—	−4.20(60)	—
η_0	−0.71510(91)	−2.97(63)	−2.75155(63)
$\eta_{D0}/10^{-5}$	—	−1.26(24)	−2.286(18)

[a] Ref. [2].
[b] Fixed at values from the microwave study by Flory et al. [2].

fine structure in CoS could be that the resolution was 0.02 cm^{-1} in the experiment for CoO [7] while the resolution was 0.04 cm^{-1} in our CoS experiment. The observed linewidths are 0.06 cm^{-1} for CoS. However, this explanation is not satisfactory since the largest linewidth for the anomalous lines in CoO is 0.1 cm^{-1} [7].

Ram et al. [7] also suggested that in CoO there is a $^4\Sigma^-$ state lying close to the $^4\Pi_i$ state because of the large Ω-doubling observed in the $^4\Pi_{3/2}$ spin component. A similar situation exists in CoS, which is supported by the Ω-doubling observed in the $^4\Pi_{5/2}$ spin component in our experiments.

The following configurations give rise to $^4\Phi$ states in CoO and CoS: $\sigma^1\delta^3\pi^3$, $\sigma^2\delta^3\pi^1\sigma^1$ and $\sigma^1\pi^4\sigma^2\delta^3\pi^3$ [8,14]. The $\sigma^2\delta^3\pi^1\sigma^1$ configuration is the only one consistent with the lack of hyperfine structure in the CoS $A^4\Phi_i$ state because the mainly Co 4$s\sigma$ orbital is filled and the unpaired σ electron is in a mainly 3$d\sigma$ orbital. However, Barnes et al. [8] proposed that the $D^4\Phi$ state of CoO observed in the visible region in their experiment arises from this configuration. High level ab initio calculations on CoO and CoS are desirable to locate all of the low-lying states and determine their configurations.

In conclusion, the $A^4\Phi_i$–$X^4\Delta_i$ and $B^4\Pi_i$–$X^4\Delta_i$ transitions of CoS have been observed for the first time in the near-infrared region using a Fourier transform spectrometer. A rotational analysis was carried out for the 0–0 bands of all four sub-bands of the $A^4\Phi_i$–$X^4\Delta_i$ transition, as well as for the 0–0, 0–1, 1–0, and 1–1 bands for the 5/2–7/2 sub-band of the $B^4\Pi_i$–$X^4\Delta_i$ transition. The analogous $^4\Pi_i$ state for CoO has been observed previously while the analogous $^4\Phi_i$ state in CoO remains to be located in the gas phase. Co nuclear hyperfine structure, which has been tentatively observed in the $^4\Pi_i$–$X^4\Delta_i$ transition of CoO, was not observed in the analogous transition of CoS. More work, both experimental and theoretical, is desirable on the low-lying electronic states of CoS and CoO.

Acknowledgment

Funding for this work was provided by the Natural Sciences and Engineering Research Council (NSERC) of Canada.

Appendix A. Supplementary data

Supplementary data for this article are available on ScienceDirect (www.sciencedirect.com) and as part of the Ohio State University Molecular Spectroscopy Archives (http://msa.lib.ohio-state.edu/jmsa_hp.htm).

References

[1] A.J. Merer, Annu. Rev. Phys. Chem. 40 (1989) 407–438.
[2] M.A. Flory, S.K. McLamarrah, L.M. Ziurys, J. Chem. Phys. 123 (2005) 164312, 1–9.
[3] C.W. Bauschlicher Jr., P. Maitre, Theor. Chim. Acta 90 (1995) 189–203.
[4] A.J. Bridgeman, J. Rothery, J. Chem. Soc. Dalton Trans. (2000) 211–218.
[5] A.G. Adam, Y. Azuma, J.A. Barry, G. Huang, M.P.J. Lyne, A.J. Merer, J.O. Schröder, J. Chem. Phys. 86 (1987) 5231–5238.
[6] D.J. Clouthier, G. Huang, A.J. Merer, E.J. Friedman-Hill, J. Chem. Phys. 99 (1993) 6336–6344.
[7] R.S. Ram, C.N. Jarman, P.F. Bernath, J. Mol. Spectrosc. 160 (1993) 574–584.
[8] M. Barnes, D.J. Clouthier, P.G. Hajigeorgiou, G. Huang, C.T. Kingston, A.J. Merer, G.F. Metha, J.R.D. Peers, S.J. Rixon, J. Mol. Spectrosc. 186 (1997) 374–402.
[9] K.C. Namiki, S. Saito, J. Chem. Phys. 114 (2001) 9390–9394.
[10] S.K. McLamarrah, P.M. Sheridan, L.M. Ziurys, Chem. Phys. Lett. 414 (2005) 301–306.
[11] M. Dolg, U. Wedig, H. Stoll, H. Preuss, J. Chem. Phys. 86 (1987) 2123–2131.
[12] G.L. Gutsev, B.K. Rao, P. Jena, J. Phys. Chem. A 104 (2000) 5374–5379.
[13] E.L. Uzunova, G.St. Nikolov, H. Mikosch, J. Phys. Chem. A 106 (2002) 4104–4114.
[14] B. Dai, K. Deng, J. Yang, Q. Zhu, J. Chem. Phys. 118 (2003) 9608–9613.
[15] D. Danset, L. Manceron, J. Phys. Chem. A 107 (2003) 11324–11330.
[16] A.B. Anderson, S.Y. Hong, J.L. Smialek, J. Phys. Chem. 91 (1987) 4250–4254.
[17] J.M. Brown, E.A. Colbourn, J.K.G. Watson, F.D. Wayne, J. Mol. Spectrosc. 74 (1979) 294–318.
[18] J.M. Brown, A.S.-C. Cheung, A.J. Merer, J. Mol. Spectrosc. 124 (1987) 464–475.
[19] R.S. Ram, J.R.D. Peers, Y. Teng, A.G. Adam, A. Muntianu, P.F. Bernath, S.P. Davis, J. Mol. Spectrosc. 184 (1997) 186–201.
[20] S. Budavari, M.J. O'Neil, A. Smith, P.E. Heckelman, The Merck Index, 11th ed., Merck & CO, Rahway, NJ, 1989.